MR Imaging and Spectroscopy in Clinical and Experimental Cerebral Ischemia: A Review

Michael Brant-Zawadzki, Philip Weinstein, Henry Bartkowski and Michael Moseley

AJNR Am J Neuroradiol 1987, 8 (1) 39-48
http://www.ajnr.org/content/8/1/39.citation

MR Imaging and Spectroscopy in Clinical and Experimental Cerebral Ischemia: A Review

Michael Brant-Zawadzki[1,2]
Philip Weinstein[3]
Henry Bartkowski[3]
Michael Moseley[1]

The superior sensitivity of MR imaging to changes in brain water caused by various insults is well established [1–6]. Because detectable alteration of brain-water content may start within the first hours after an ischemic insult [7, 8], MR imaging promises to be a unique tool in the experimental and clinical approach to cerebral infarction. MR spectroscopy offers a noninvasive method for observing the fundamental metabolic processes of cell function. Phosphorus-31 (P-31) MR spectroscopy can elucidate the accumulation and depletion of molecules that act as the energy storage substrates of the cell and their breakdown products. The pH within the tissue of interest can be calculated. Hydrogen MR spectroscopy can detect lactate accumulation when ischemia forces a shift from aerobic to anaerobic glycolysis. More sophisticated metabolic pathways are also accessible to MR spectroscopy. Because MR imaging and MR spectroscopy can be done with the same instrument in a single experimental model or in a human patient, MR offers a unique methodology for investigating acute (potentially reversible) ischemia, its evolution, and the effect of various therapeutic interventions on its prognosis.

The purpose of this review is to summarize the initial experience with MR imaging in the clinical setting of cerebral ischemia and to introduce the reader to the potential future application of combined MR imaging/spectroscopy in this disease process by discussing clinically relevant experimental models. A brief overview of the basic principles of MR spectroscopy is included. A broad understanding of the pathophysiology of ischemia is vital to the task at hand and is a good starting point for subsequent discussion.

Cerebral Ischemia: Pathophysiology

It should be emphasized at the start that a dissociation between the pathophysiology of ischemia and its clinical expression often occurs. That is, even when permanent tissue damage (i.e., infarction) occurs, the clinical neurologic deficit may be either nonexistent, transient, or permanent to varying degrees. Therefore, strict adherence to proper terminology is important in any discussion of ischemic phenomena.

Cerebral ischemia results when either general or focal reduction of blood flow to the brain occurs. If such reduction of flow is of sufficient magnitude and duration, irreversible cellular changes leading to cell death ensue. Hypoxia and hypoglycemia may produce similar effects despite intact cerebral perfusion, but these specific insults are beyond the scope of the current discussion and, as such, will not be considered.

Global reduction of cerebral blood flow generally results from extracranial events, such as significant loss in cardiac output due to muscle damage, arrhythmia, massive central vessel thrombosis, or diffuse occlusive disease in the carotid and vertebrobasilar system. If perfusion is lowered diffusely, compensatory collateral pathways are themselves affected and unavailable. Most often, however, cerebral

This article appears in the January/February 1987 issue of *AJNR* and the March 1987 issue of *AJR*.

Received June 16, 1986; accepted after revision August 4, 1986.

[1]Department of Radiology, University of California, San Francisco, CA 94143.

[2]Present address: Newport Harbor Radiology Associates, 355 Placentia, Suite 207, Newport Beach, CA 92663. Address reprint requests to M. Brant-Zawadzki.

[3]Department of Neurosurgery, University of California, San Francisco, CA 94143.

***AJNR* 8:39–48, January/February 1987**
0195-6108/87/0801-0039

ischemia is a regional event in the distribution of one of the three major vascular territories and is due to a combination of factors, including the efficiency of the heart's pumping action in providing flow, the state of the vessels delivering it, and the character of the circulating medium (i.e., blood-oxygen carrying capacity, viscosity, coagulability). Most cerebral infarctions are due to coexisting changes in several of these factors.

Once regional cerebral blood flow (rCBF) drops below a critical threshold (10–20 cc/100g/min), a number of biochemical alterations are triggered in the ischemic tissue. The subsequent rapid shifts in electrolyte and water concentrations between the intra- and extracellular compartments have been investigated in a number of elegant experimental models [7–13]. The brain normally extracts 50% of the oxygen and 10% of the glucose available from blood for energy production. With ischemia, therefore, there is initially a relative lack of oxygen but not glucose, and the reduced energy production from oxidative phosphorylation can for a time be counteracted by increased glycolysis. However, the progressive loss of oxygen necessitates anaerobic glycolysis, which yields much less adenosine triphosphate (ATP) and produces increasing amounts of lactic acid. Any residual flow delivers only a limited amount of oxygen, given the tissue needs, but sufficient glucose. This tissue hyperglycemia raises tissue osmolality, fuels the lactic acid production, and depletes the ATP available for maintaining electrolyte hemostasis within the cell. Release of ions from intracellular binding sites occurs, the Na/K pump (fueled by ATP) fails, extracellular Na goes into the cells, K leaks out. Of interest, sodium and water fluxes parallel each other in the first few hours [9]. Water begins to accumulate within the cell due to the osmotic gradient caused by the increased lactate and sodium levels. Phospholipid catabolism occurs during early ischemia, leading to free fatty acid accumulation. The free fatty acids increase tissue osmolality further, more water shifts from the capillary space into the affected tissues, and the local acidosis (lactic and fatty acids) destroys mitochondria. All this occurs within the first 30 min of ischemia. Further progression of these events leads to extensive damage to mitochondrial and cytoplasmic membranes as well as to those of vascular endothelium. By 6 hr, the blood-brain barrier (BBB) begins to break down, with subsequent leakage of water and protein from the intravascular compartment. The above-described mechanisms yield early intracellular (cytotoxic) edema on the basis of redistribution of water from the microcapillary and extracellular-to-intracellular spaces, but some (approximately 3%) overall increase in total water is seen within the first hour or so. When flow drops to zero, the lack of continued vascular supply precludes any further increase in water within the tissue as a whole. Conversely, reperfusion of severely ischemic tissue, either by the native routes or via established (as often happens in vivo) collaterals, may significantly aggravate the degree of edema formation, especially of the extracellular space. The degree of this type of edema formation (vasogenic) is dependent somewhat on persistent perfusion of the region. The resulting mass effect may compromise the microcirculation, including that in the zone just adjacent to the severely ischemic region, and this border zone (penumbra) may itself progress to irreversible ischemia. Because reperfusion can reverse ischemia within the first 30 min of onset but may aggravate the situation if instituted later, the value and timing of such therapy is controversial.

Given the above sequence of events, the factors that will most affect the MR images relate to the initially slight increase in overall tissue-water content associated with early cytotoxic edema, followed by the more massive water accumulation of the vasogenic phase. The degree of protein leakage associated with this latter phase may modify the initial prolongation of T1 and T2 relaxation effects, and will correlate with the degree of enhancement produced by paramagnetic agents, themselves large proteinaceous molecules.

The more basic mechanisms of early ischemia, easily amenable to study with MR spectroscopy, include the acute depletion of ATP, accumulation of inorganic phosphates, lactic acid production, and calculation of tissue pH. It may eventually be possible to monitor levels of certain fatty acids and even track glucose utilization in certain experimental models of brain ischemia.

The further pathologic evolution of acute ischemia is also important to understand for imaging purposes. The edematous mass effect of infarction is greatest in the first week, but it should be resolving by the third week. Petechial hemorrhage occurs in up to 40% of cases, usually in the second week, and is most often clinically occult [14]. The residual tissue will become atrophied, soft (due to fewer cellular elements and greater water content), and will show gliosis. If hemorrhage accompanied the infarct, hemosiderin staining may be evident in the residual tissue. Frankly cystic foci may be seen after small infarcts and, rarely, dystrophic calcification of infarcted brain may occur.

Given this brief overview of the pathophysiology of acute cerebral ischemia and its evolution, manifestations of this process on clinical and experimental MR studies can now be better understood.

MR Imaging of Cerebral Ischemia

The major advantage of proton MR imaging in evaluating cerebral ischemia is this technique's superior sensitivity to the insult. This should not be surprising given the fact that water accumulates within the first hours of the onset of cerebral ischemia, and each water molecule has two hydrogen nuclei that provide the MR signal. Not surprisingly, most clinical studies document the improved ability to detect infarction with MR as compared with CT [15–23]. Indeed, experimental models of cerebral infarction have shown that MR can detect the changes associated with ischemia in the first 2 hr after vascular occlusion [24, 25]. In our own laboratory, cats with middle cerebral artery occlusion (MCA-O) showed changes consistent with ischemia within the first hour in two of five instances. Ischemia beyond 6 hr in duration was routinely demonstrated [26].

As expected from the pathophysiologic events described, the T1 and T2 relaxation parameters that are responsible for signal-intensity alterations are both prolonged. In fact, experimental evidence suggests that T1 and T2 prolongation is greatest in the earliest stages of ischemia, when bulk water accumulates, and before opening of the BBB to macromolecules. At this early time, low intensity should

be seen on T1-weighted images, and high intensity on T2-weighted ones. The latter prove more sensitive to infarction, because some T2 effect is impossible to avoid on T1-weighted sequences [1] (Figs. 1 and 2). An influx of protein into the edematous region serves to decrease somewhat the abnormally prolonged T1 and T2 relaxation values [26] and, in turn, may modify the imaged signal intensity. It has been suggested that sodium MR imaging might offer unique advantages in the evaluation of infarction given the early accumulation of sodium in ischemic tissue [27]. However, because water and sodium shifts parallel each other in acute ischemia, and proton MR imaging is so sensitive, the clinical value of sodium MR imaging in this setting seems limited.

The great sensitivity of MR imaging to acute ischemia both in the experimental and clinical experience suggests that reversible, transient alterations might be detectable. Such reversibility of acute ischemia has been documented in an experimental model providing that reperfusion of the ischemic region occurs before the onset of permanent damage [7]. Clinical experience has shown reversibility of MR imaging changes thought to be due to ischemia in patients with vasculitis secondary to systemic lupus erythematosus [21].

Fig. 1.—Cerebellar infarction, 16 hr.
***A*, CT scan shows equivocal low density in left cerebellar hemisphere; study degraded by streak artifact.**
***B*, T2-weighted (SE 2000/60) 0.35-T MR image shows abnormally high signal throughout left cerebellar hemisphere as well as in periphery of right cerebellar hemisphere.**

Contrast enhancement with paramagnetic Gd-DTPA depends on development of BBB breakdown [28]. Enhancement with this contrast agent was seen first at 16–18 hr (rate of accumulation) in our experimental model [29]. Of note, the wash-in of contrast in this same model was greatest in the first 24–72 hr. At a later stage, when a significant amount of vasogenic edema was present in the infarcted brain, the wash-in of contrast was slow. This slow inflow correlated with the greatest phase of edema and mass effect. Presumably, microvascular compromise due to that mass effect precluded rapid inflow of contrast agent (and, by extension, of blood nutrients).

The ability of MR imaging to separate acute hemorrhage from edema has been suboptimal within the first few days of a clinically manifest cerebrovascular accident. Both infarction and hemorrhage tended to show a high signal on T2-weighted images, with variably low to isointense signal on T1-weighted images (Fig. 3). More recently, preferential T2 shortening has been shown in acute hemorrhage, especially noticeable at high fields [30]. Such T2 shortening is especially evident in high-field images as a focus of low signal intensity in acute hemorrhagic foci on T2-weighted images (Fig. 4). Further experience with acute hemorrhage at various field strengths is necessary to convincingly prove that MR imaging can distinguish acute hemorrhage and ischemia in all instances.

On the other hand, subacute hemorrhage within infarction is sensitively documented by MR imaging. Many bland infarcts have at least some microscopic and CT evidence of petechial hemorrhage if looked for [14]. It is likely, that given the paramagnetic effects of methemoglobin, such small foci of hemorrhage may be more sensitively detected with MR imaging (Fig. 5). Because the controversy regarding anticoagulation of patients with recent infarction continues [31], such improved sensitivity of MR imaging may add fuel to the discussion.

Other limitations of MR imaging in the evaluation of cerebral ischemia exist. Because the gray matter has a significantly greater water content than the white matter, small infarcts within the cortical mantle may be difficult to identify in the early stages. This is especially true when the slice thickness and image matrix are coarse, and

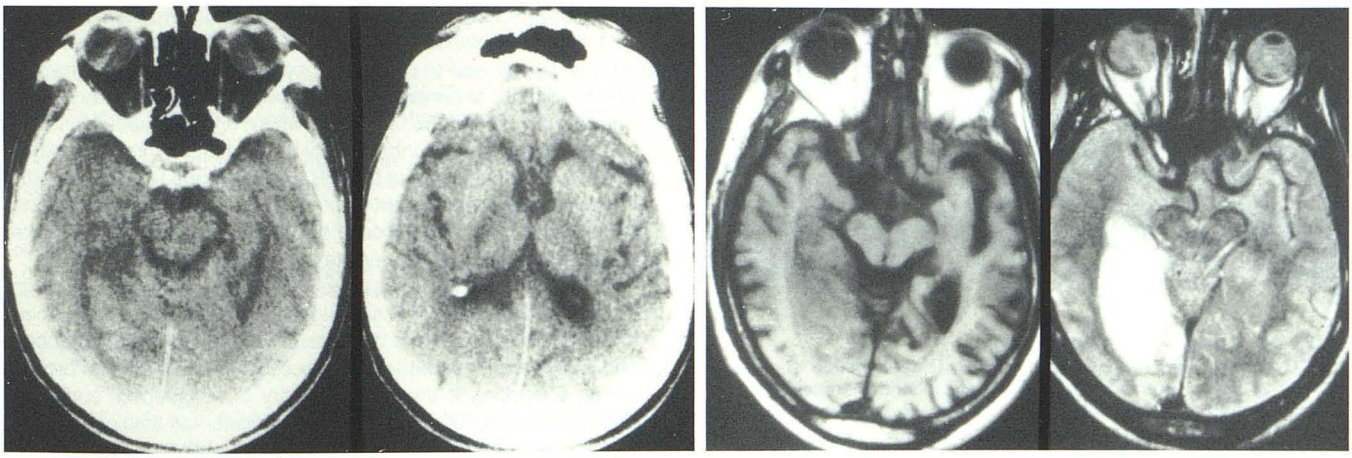

Fig. 2.—Acute onset of left homonymous hemianopsia and weakness 12 hr before imaging.
***A*, CT study shows vague foci of low density in distribution of right posterior cerebellar artery on two adjacent sections.**
***B*, T1-weighted (SE 500/30) and T2-weighted (SE 2000/60) 0.35-T images (left and right, respectively) from MR scan done just after CT at same level. Note superior depiction of large infarcted region with T2-weighted study.**

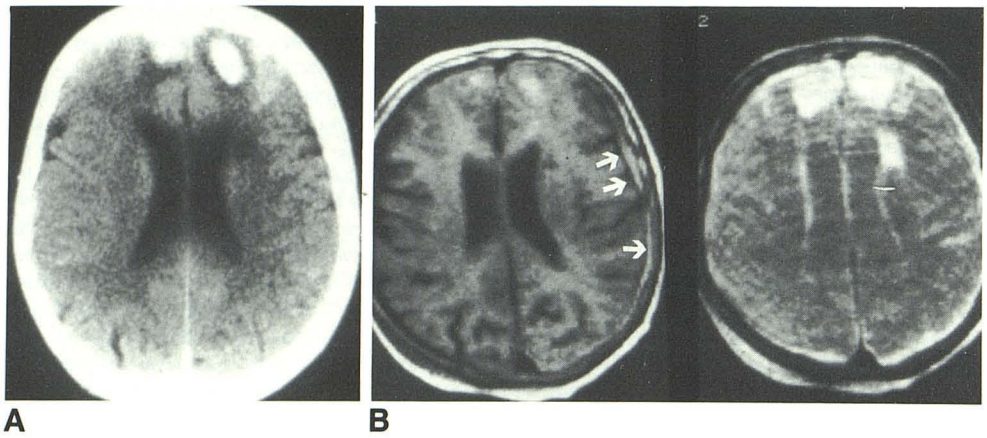

Fig. 3.—Acute bifrontal hematomas (8 hr); old left caudate infarct.

***A*, CT scan shows the two hematomas as high-density foci.**

***B*, T1-weighted (SE 500/30) and T2-weighted (SE 2000/60) 0.35-T images (left and right, respectively) obtained just after the CT. Note that intensity of left subdural hematoma (*arrows*) matches that of white matter with SE 500/30, so that focal bifrontal hematomas are not distinguishable. With SE 2000/60, these hematomas show high signal, but one matching that of caudate infarct.**

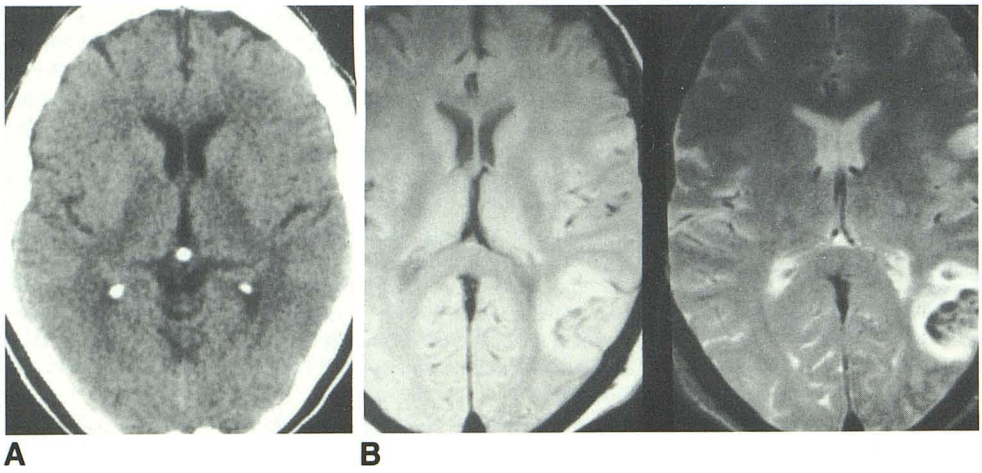

Fig. 4.—Acute infarct with secondary hemorrhage.

***A*, CT scans at 8-hr after onset of aphasia is negative.**

***B*, Two echoes of a T2-weighted (SE 2000/40, 80) sequence done on a 1.5-T unit at day 1 when patient was still aphasic but excessively anticoagulated show preferential T2 shortening (low signal) within left temporal infarct. Clinical course was that of typical cerebral infarct.**

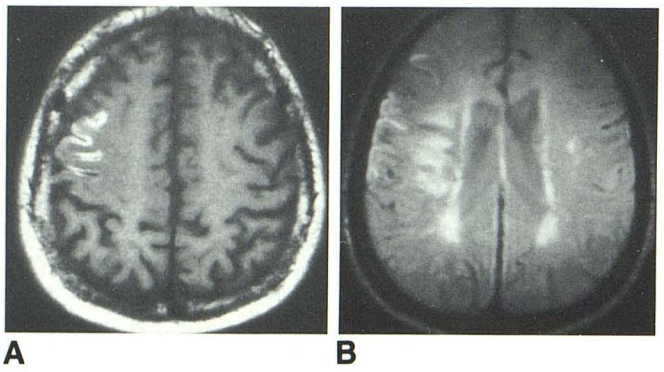

Fig. 5.—Subacute infarct with hemorrhage.

***A*, Gyriform pattern of high signal intensity is seen on this T1-weighted (PS 600/25) image in a patient with right hemispheric infarction.**

***B*, More extensive abnormality due to edema is seen on T2-weighted, 1.5-T images (SE 2000/80) in infarcted region.**

partial-volume artifact becomes a problem. Also difficult for MR imaging is the phenomenon of luxury perfusion. This refers to the presence of arteriovenous shunting of blood in the peripheral zone of infarction, shown by angiography or contrast-enhanced CT as a cortical blush. MR imaging has difficulty depicting flow in the capillary space. The normal intravascular volume represents only 4–7% of the overall brain volume. Therefore, the flow within the capillary space, or its absence, contributes little overall signal on routine MR imaging within any given volume of interest. Indeed, even when paramagnetic contrast agents are injected, the capillary space does not visibly enhance [32]. Therefore, unlike CT, where enhancement can be due to either intravascular contrast or its extravasation through a broken BBB, contrast enhancement in MR imaging does not appear within the vascular space on the arterial side of the circulation under normal circumstances, and the vascular blush of luxury perfusion will likely be missed on MR imaging despite use of intravenous Gd-DTPA.

The sensitivity of MR imaging to the edema produced by infarction is of tremendous value in assessing the acute stages of the process, when the clinical picture is consistent with the MR imaging appearance. However, most pathologic processes in the brain can produce edema. Therefore, if the clinical history is nonspecific, and/or the pattern of distribution of edema is not typical for that of infarction, the diagnosis may be difficult to ascertain (Fig. 6).

Atypical location for infarction may occur with ischemia due to causes other than the typical embolic phenomena seen in atherosclerotic disease. For example, vasculitides produce ischemia in the multifocal distribution of the small arterioles at the gray-white junction, whereas a spasm due to subarachnoid hemorrhage and other causes of global hyperperfusion tend to affect the watershed regions most

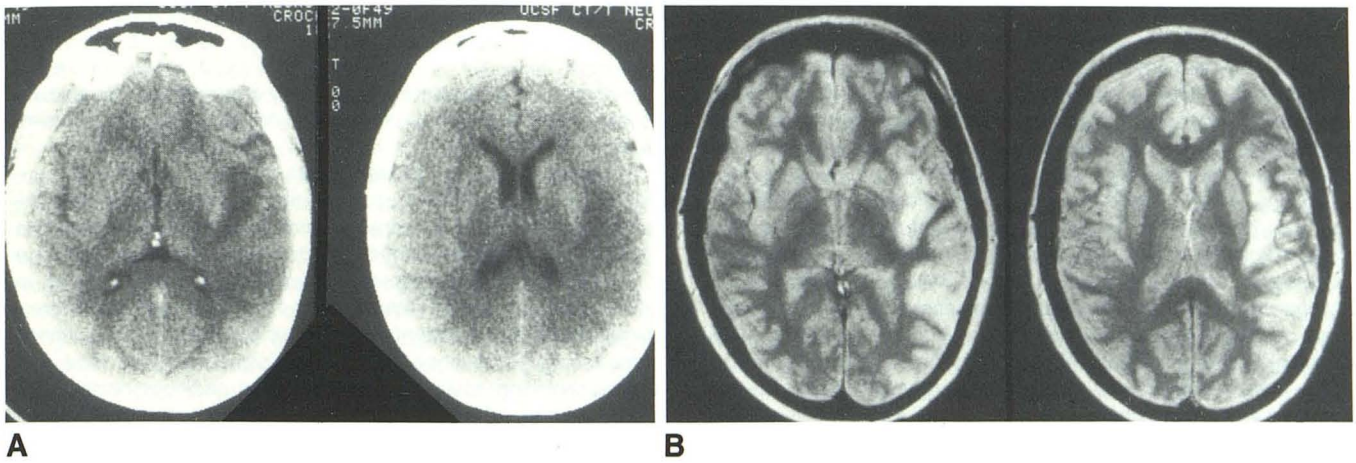

Fig. 6.—Suspected brain tumor in middle-aged woman with 2-week history of confusion.

A, CT at two adjacent levels shows well-circumscribed, low density in sylvian region, with subtle mass effect.

B, MR (SE 2000/60) 0.35-T image at corresponding levels shows high signal in abnormal region consistent with increased water content. The nonspecific history and persistence of abnormal CT findings prompted biopsy for suspected neoplasm. A subacute infarct was seen histologically.

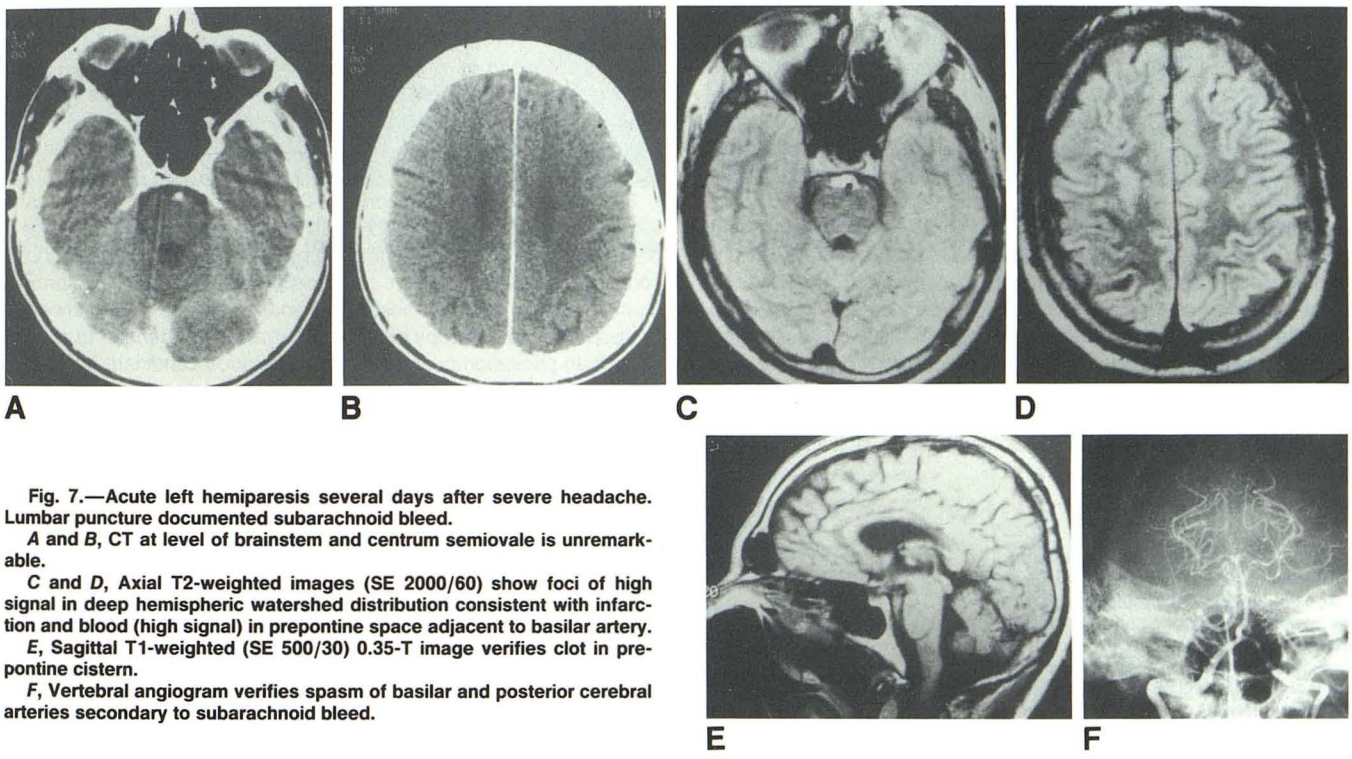

Fig. 7.—Acute left hemiparesis several days after severe headache. Lumbar puncture documented subarachnoid bleed.

A and *B*, CT at level of brainstem and centrum semiovale is unremarkable.

C and *D*, Axial T2-weighted images (SE 2000/60) show foci of high signal in deep hemispheric watershed distribution consistent with infarction and blood (high signal) in prepontine space adjacent to basilar artery.

E, Sagittal T1-weighted (SE 500/30) 0.35-T image verifies clot in prepontine cistern.

F, Vertebral angiogram verifies spasm of basilar and posterior cerebral arteries secondary to subarachnoid bleed.

typically (Fig. 7). In questionable cases of appearance or distribution, it is best to wait for the temporal evolution of acute infarction to manifest itself. For example, if 3 or 4 weeks go by and the lesion in question is not diminishing in its mass effect, and certainly if it is enlarging, another process must be sought as the explanation for the MR imaging abnormality.

Old infarcts may show regions of focal cystic change in the brain, exhibiting marked prolongation of T1 and T2 relaxation values. In such cases, the structure affected is generally atrophic. However, not all old infarcts are cystic. In fact, chronic ischemic foci may simply show areas of focal encephalomalacia: loose stroma in the brain with increased water content, and associated gliosis. Such lesions are quite typical of the population over age 65. Autopsy studies show that small infarcts in the deep portions of the brain are the commonest finding at autopsy in otherwise normal patients [33, 34]. MR imaging reflects this fact in that 20–30% of patients over age 65 show

multifocal regions of high signal intensity on T2-weighted images consistent with edema and/or demyelination [35].

The pathophysiology of the aging brain helps shed some light on the possible etiologies behind these deep, patchy white-matter lesions. In the normal adult, the perfusion to the cortical mantle is threefold that to the deep hemispheric white matter, the latter being dependent on relatively sparse, long, and thin perforating vessels. With aging, cerebral blood flow diminishes diffusely [36–38]. Therefore, the effects of the diminished cerebral perfusion with advancing age are probably first felt in the deep hemispheric portions, given the relative lower flow to this region to begin with. It is not too far fetched to suppose that with superimposed hypotensive episodes, perhaps some degree of extracranial cerebrovascular occlusive disease, or intracranial small-vessel disease, the threshold for ischemic change in the deep hemispheric white matter is reached. It is also not surprising that most of these infarcts are silent. Even large, vascular distribution infarctions may occasionally produce no or minimal symptomatology. Transient ischemic attacks are, by definition, reversible clinical events. But their pathologic counterpart may be permanent [39]. Therefore, the high frequency of high-signal abnormalities on T2-weighted MR images in the deep hemisphere in the brains of asymptomatic, normal elderly people may well represent diffuse ischemic change. Such abnormalities have anecdotally shown an association with cerebrovascular disease risk factors, and even dementia [40]. Because multiinfarct dementia is the second commonest cause of cognitive loss in the elderly, the impact of MR imaging on investigations of the aging brain should be significant.

In summary, then, the major strength of MR imaging in evaluating cerebral ischemia is in the sensitivity that it provides for detecting the disease process. This advantage must be tempered by the realization that edema is a nonspecific event related to various insults affecting the brain, as well as the still uncertain ability of MR imaging, at least at the lower field strengths, to separate acute hemorrhagic from acute ischemic events. The superior sensitivity of MR imaging should help in investigations aimed at evaluating various forms of intervention in acute ischemia. Whether reperfusion, antiedema agents, or calcium channel blocking agents (which affect the early electrolyte shifts in acute ischemia) can ameliorate some of the damage caused by ischemia remains to be seen. Because some of these acute changes are at a fundamental level of biochemistry, proton MR imaging may be insufficient to explore the numerous variables. For this reason, the potential offered by MR spectroscopy in cerebral ischemia research and possibly in clinical settings is worth discussing, at least briefly.

MR Spectroscopy in Cerebral Ischemia

Before launching into some of the early experience in this area, let us briefly review the basic principles of MR spectroscopy in a simplistic fashion.

MR imaging and spectroscopy share the same fundamental principles and instrumentation, leading to the eventuality that both techniques can be done in the same machine. In essence, MR imaging is a sophisticated adaptation of MR spectroscopy. One major difference in the data acquisition process distinguishes the two techniques. In MR imaging, the operator changes the homogeneity of the external magnetic field in a predetermined pattern in order to produce a change in the resonant frequency of the nuclear signal being sampled, that change providing spatial localization for the particular nucleus. On the other hand, MR spectroscopy requires a homogeneous external magnetic field in the region of interest. Any deviation from the expected resonant frequency for a nucleus must reflect microenvironmental magnetic field gradients induced by the chemistry of the tissue (Fig. 8). These local gradients are of a much smaller order of magnitude than the predetermined gradient produced in MR imaging. The local gradients result mostly from the groupings of electrons (electron clouds) around the target nuclei within the molecule in which these nuclei reside. As a result, each particular nucleus sees a slightly different magnetic field and resonates with the frequency reflecting that locally altered magnetic field, and not the frequency with which the nucleus would resonate were the external field totally homogeneous and not influenced by the local microenvironment. By measuring this change in resonant frequency from the ideal, we can determine the type of molecule the nucleus is in, and even the various positions of the given nucleus within the same molecule, because the electron clouds will vary in configuration and effect from place to place.

For example, with phosphorus (P-31) MR spectroscopy, one can identify different resonant frequencies from the various terminal phosphorus nuclei in ATP. The separation of ATP from other phosphorus-containing molecules—such as phosphocreatine, inorganic phosphate moieties, phosphodiesterase, and so on—is easily accomplished. MR spectroscopy can be performed with attention to nuclei other than phosphorus, and hydrogen is a good candidate for spectroscopy as well as imaging. Hydrogen (H-1) spectroscopy can allow the detection of lactate, an important product of anaerobic glycolysis. Other nuclei—such as carbon-13, fluorine-19, sodium-23, and so

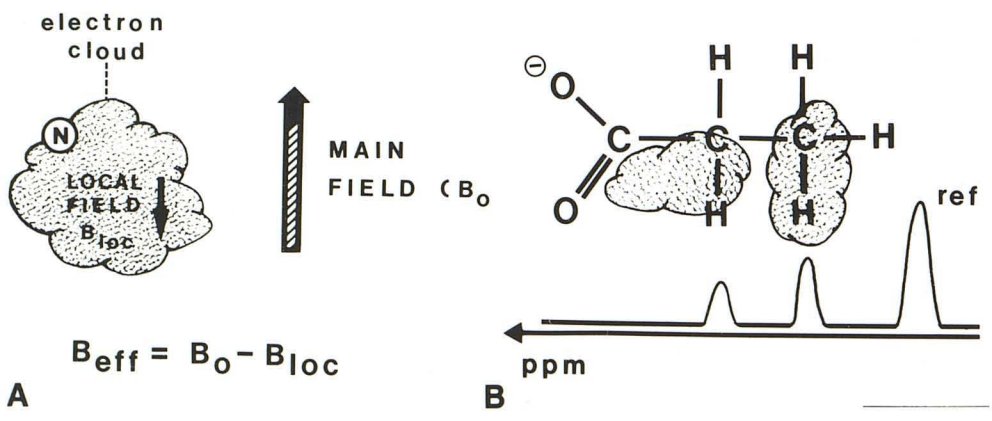

Fig. 8.—Schematic representation of the chemical shift principle: see text.

***A*, The nucleus (N) should resonate at a frequency set by the homogeneous external magnetic field B_o. The presence of local tissue magnetic field due to imaging electrons (B loc) produces a slightly different effective field seen by the nucleus; this causes a slight alteration of the resonant frequency from that expected in B_o alone.**

***B*, An illustrative molecule examined with hydrogen spectroscopy. Despite identical external field (B_o), each hydrogen nucleus resonates with a slightly different frequency from that of the reference, due to distinct configurations of the electron cloud produced by the molecule's configuration. The change in frequency is expressed as a ratio—parts per million (ppm).**

on—can also be used for spectroscopy. However, in terms of cerebral ischemia, P-31 and H-1 spectroscopy have been the two nuclei with which MR spectroscopy has been done in the initial stages of evaluating in vivo spectroscopy of cerebral ischemia.

Most experience in this area has been derived from well-controlled studies of global cerebral hypoxia [41–43]. Basically, P-31 spectroscopy shows the depletion of high-energy phosphates (ATP and phosphocreatine) with progressive global hypoxia, accumulation of inorganic phosphates, and a lowered pH due to acidosis in the ischemic tissue. Lactic acid accumulation has been documented with progressive ischemia using H-1 spectroscopy.

Because most clinical cerebral ischemic lesions are focal rather than global, we have begun evaluating MR spectroscopy and imaging in a single instrument using both hemispheric and regional cerebral infarction models. What we have noted is dissociation between the information provided by the imaging and spectroscopy techniques, as well as their relationship to the clinical state of the animal.

For example, we have evaluated infarction in the mongrel dog brain. By surgical occlusion of all six vessels leading to one hemisphere, a global hemispheric infarct can be produced. This is seen on T2-weighted MR imaging 24 hr after the injury as a panhemispheric region of high signal intensity consistent with edema (Fig. 9). The midline shift accompanies the finding. Spectroscopy obtained at the same time shows a single large inorganic phosphate peak that is consistent with total devitalization of the organ (Fig. 10).

On the other hand, surgical occlusion of only three vessels allows more regional ischemia to occur, with preservation of collateral perfusion. In such a model, the initial spectra are more ominous than the MR images (Fig. 11). The imaging shows only slight suggestion of high signal intensity in the affected hemisphere (Fig. 12) whereas the spectra already show marked depletion of the high-energy phosphates and a shift of inorganic phosphate indicating lowered pH in the first hours of infarction. Lactate levels were studied with hydrogen MR spectroscopy at the same time the phosphorus spectra were obtained, and showed accumulation in concert with the decreased high-energy phosphate levels.

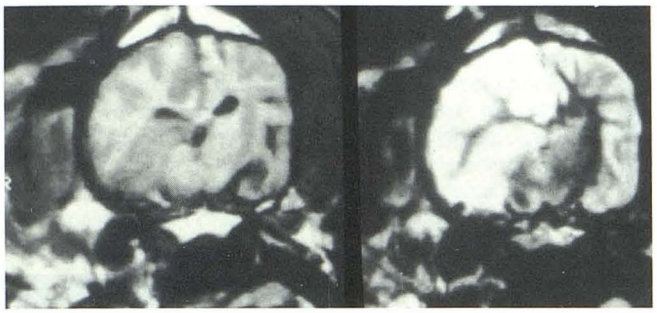

Fig. 9.—Experimental global hemispheric infarct in dog—24 hr.T1-weighted (*left*) and T2-weighted (*right*) images shows midline shift and high signal on T2-weighted image throughout right hemisphere.

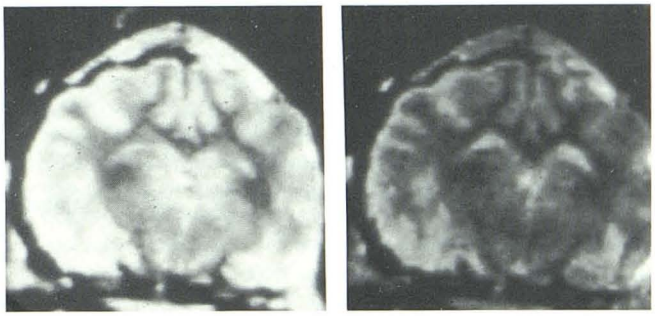

Fig. 11.—Regional cerebral infarct in dog with collateral perfusion—5 hr. T2-weighted images (SE 2000/30, 60) show equivocal changes only.

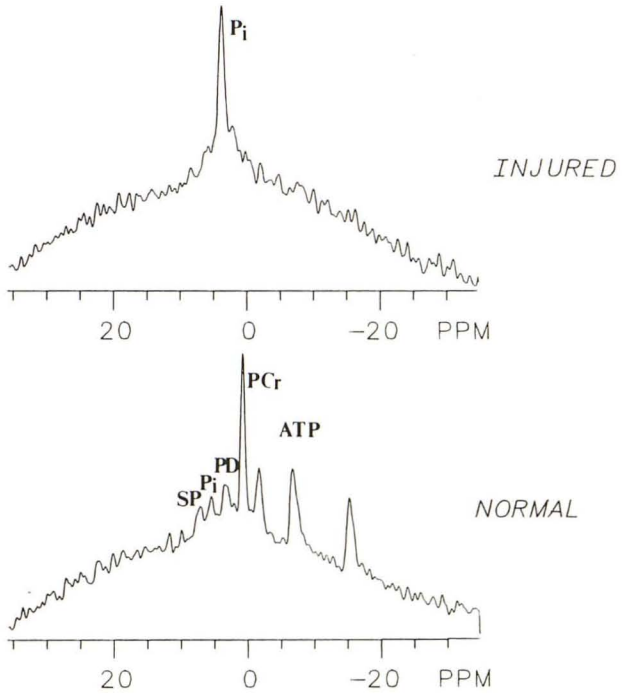

Fig. 10.—P-31 of hemispheric ischemia in dog's brain 24 hr after injury. Spectroscopy in the same experiment as in Fig. 9 shows only a high inorganic phosphate peak on the injured side versus the normal phosphorus spectrum (*bottom*) on the normal side (see text). (P_i = inorganic phosphate; ATP = adenosine triphosphate; PCr = phosphocreatine; PD = phosphodiesters; SP = sugar phosphates.)

```
BETH      004
MM        18JUL85

24 HOUR ISCHEMIA NORMAL SIDE

PREPULSE P2=90 P5=30 D12 1U QP1

P2        =  110.00 USEC
P5        =   36.60 USEC
D5        =    2.00  SEC
D12       =     .00 USEC
NA        =     128
SIZE      =    4096
ADC       =      12
AI        =       2
RG        =      40
SW        =  +/- 3012.04  HZ
DW        =   166 USEC
DE/DW     =    .80
AT        =  339.97 MSEC
F2        =  500.058852
OF        =  288.26
SF        =  34.631002
PA        =  290.7
PB        =   12.2
LOCK      =    4.80

OBS HI PWR =  63
OBS LO PWR =  200
DEC PWR    =  0
DEC SCHEME =  4
SCALE      =  245.31 HZ/CM
           =  7.0837 PPM/CM

FROM       35.84
TO       -34.90 PPM
```

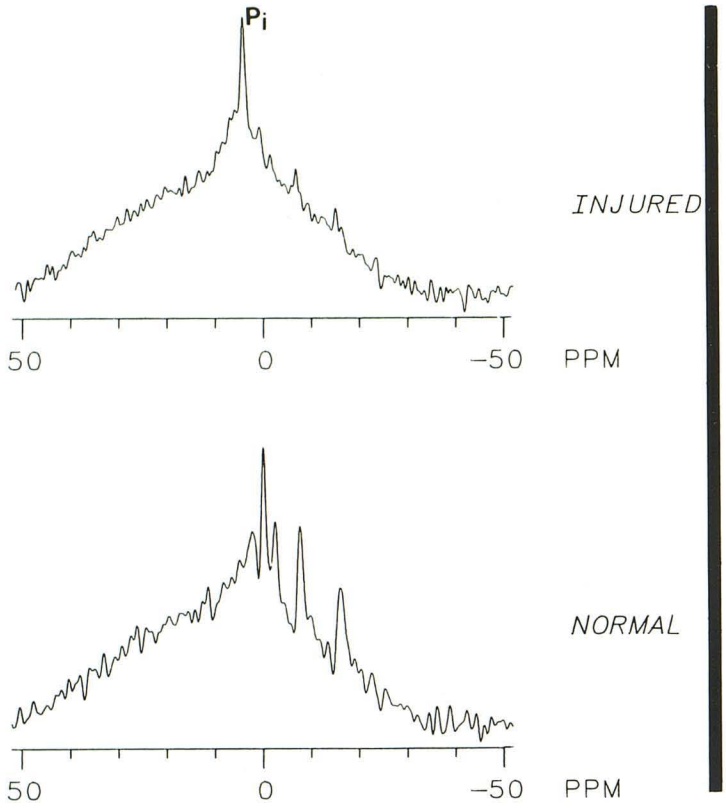

Fig. 12.—P-31 of unilateral ischemia in dog's brain 5 hr after occlusion. Spectroscopy in same experiment as in Fig. 11 shows depletion of high-energy phosphates and elevation with shift of inorganic phosphate peak in abnormal hemisphere (*top*) when compared with normal side (*bottom*).

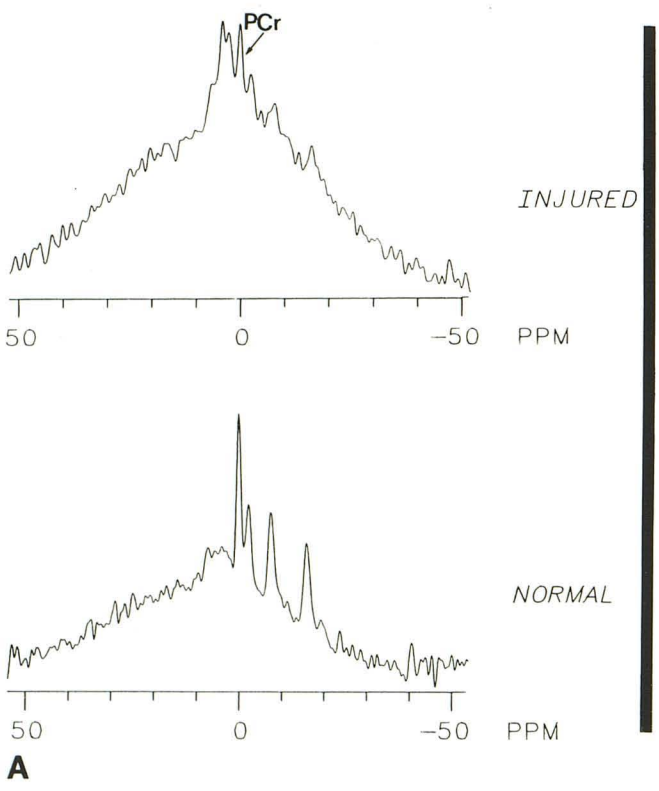

A

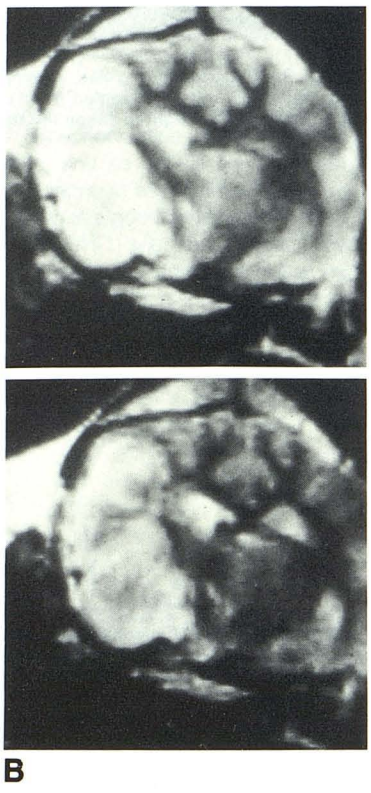

B

Fig. 13.—Imaging and spectroscopy repeated in same animal as in Figs. 11 and 12 at 30 hr.

***A*, P-31 of unilateral ischemia in dog's brain 30 hr after occlusion. Spectra from abnormal side (*top*) are more normal in appearance when compared with study 24 hr earlier—compare with Fig. 12 (see text).**

***B*, T2-weighted images (SE 2000/30, 60) now show large area of high signal due to infarction.**

This same animal was studied 25 hr later. The MR images became much more abnormal (Fig. 13); however, the spectra were returning toward normal. In fact, clinically, the animal appeared somewhat improved at this time. Nevertheless, death ensued several hours later. Such data can be interpreted in several ways. Clearly, in the initial phases of ischemia, the spectroscopy appeared more sensitive than imaging in this particular experiment. Subsequently, the images suggested a more ominous insult than one that would correspond to the now resolving spectra. Two possibilities may explain this phenomenon. On the one hand, MR spectroscopy may reflect the improving picture of the animal neurologically. More likely, however, is the fact that with maintained collateral perfusion over the 25-hr interval between the first and second study, the abnormal tissues have been totally devitalized and the abnormal metabolites have been washed out through collateral perfusion. Left behind are the remnant, viable cells with normal metabolism detected by spectroscopy. The progressive edema occurring through the sites of BBB breakdown, driven by the collateral perfusion to the region, eventually causes further ischemia and subsequently sufficient mass effect to produce the animal's death.

This early anecdotal experience points out that a great deal still needs to be learned about MR spectroscopy and imaging in combination. Specifically, the biggest current hurdle is obtaining spectra from a localized, small region of interest. Until this is available, there is always the probability that partial-volume effects of spectra from normal as well as abnormal tissue will be obtained. Nevertheless, the potential of spectroscopy in evaluating acute intervention and therapy in the early stages of ischemia—or possibly subclinical, potentially reversible, chronic ischemia—is clear. It is this hope that drives the further development of combined MR imaging and spectroscopy to its logical extent.

REFERENCES

1. Brant-Zawadzki M, Norman D, Newton TH, et al. Magnetic resonance of the brain: the optimal screening technique. *Radiology* **1984**;152:71–77
2. Bradley WG, Waluch V, Yadley RA, Wycoff RR. Comparison of CT and MR in 400 patients with suspected disease of the brain and cervical spinal cord. *Radiology* **1979**;152:695–702
3. Bydder GM, Steiner RE, Young IR, et al. Clinical NMR imaging of the brain: 140 cases. *AJNR* **1982**;3:459–480
4. Brant-Zawadzki M, Badami JP, Mills CM, Norman D, Newton TH. Primary intracranial tumor imaging: a comparison of magnetic resonance and CT. *Radiology* **1984**;150:435–440
5. Naruse S, Horikawa Y, Tanaka C, Hirakawa K, Nishikawa H, Yoshizaki K. Proton nuclear magnetic resonance studies on brain edema. *J Neurosurg* **1982**;56:747–752
6. Brant-Zawadzki M, Bartkowski HM, Ortendahl DA, et al. NMR in experimental and clinical cerebral edema. *Noninvasive Med Imag* **1984**;1:43–47
7. Bell BA, Symon L, Branston NM. CBF and time thresholds for the formation of ischemic cerebral edema, and effect of reperfusion in baboons. *J Neurosurg* **1985**;62:31–41
8. Iannotti F, Hoff JT, Schielke GP. Brain tissue pressure in focal cerebral ischemia. *J Neurosurg* **1985**;62:83–89
9. Gotoh O, Asano T, Koide T, Takakura K. Ischemic brain edema following occlusion of the middle cerebral artery in the rat. I: The time courses of the brain water, sodium and potassium contents and blood-brain barrier permeability to ^{125}I-Albumin. *Stroke* **1985**;16(1):101–109
10. Hossmann K-A, Schuier FJ. Experimental brain infarcts in cats. I. Pathophysiological observations. *Stroke* **1980**;11(6):583–592
11. Schuier FJ, Hossmann K-A. Experimental brain infarcts in cats. II. Ischemic brain edema. *Stroke* **1980**;11(6):593–601
12. Marcy VR, Welsh FA. Correlation between cerebral blood flow and ATP content following tourniquet-induced ischemia in cat brain. *J Cereb Blood Flow Metab* **1984**;4:362–367
13. Welsh FA. Review regional evaluation of ischemic metabolic alterations. *J Cereb Blood Flow Metab* **1984**;4:309–316
14. Horning CR, Dorndorf W, Agnoli AL. Hemorrhagic cerebral infarction: a progressive study. *Stroke* **1986**;17:179–184
15. Bryan RN, Willcott MR, Schneiders NJ, Ford JJ, Derman HS. Nuclear magnetic resonance evaluation of stroke: a preliminary report. *Radiology* **1983**;149:189–192
16. Sipponen JT. Uses of techniques: visualization of brain infarction with nuclear magnetic resonance imaging. *Neuroradiology* **1984**;26:387–391
17. Kistler JP, Buonanno FS, DeWitt LD, Davis KR, Brady TJ, Fisher CM. Vertebral-basilar posterior cerebral territory stroke—delineation by proton nuclear magnetic resonance imaging. *Stroke* **1984**;15(3):417–426
18. Pykett IL, Buonanno FS, Brady TJ, Kistler JP. True three-dimensional nuclear magnetic resonance neuro-imaging in ischemic stroke: correlation of NMR, x-ray CT and pathology. *Stroke* **1983**;14(2):173–177
19. Sipponen JT, Kaste M, Ketonen L, Sepponen RE, Katevuo K, Sivula A. Serial nuclear magnetic resonance (NMR) imaging in patients with cerebral infarction. *J Comput Assist Tomogr* **1983**;7(4):585–589
20. Brant-Zawadzki M, Solomon M, Newton TH, Weinstein P, Schmidley J, Norman D. Basic principles of magnetic resonance imaging in cerebral ischemia and initial clinical experience. *Neuroradiology* **1985**;27(6):517–520
21. Aisen AM, Gabrielsen TO, McCune WJ. MR imaging of systemic lupus erythematosus involving the brain. *AJNR* **1985**;6:197–201
22. Vermess M, Bernstein RM, Bydder GM, Steiner RE, Young IR, Hughes GRV. Nuclear magnetic resonance (NMR) imaging of the brain in systemic lupus erythematosus. *J Comput Assist Tomogr* **1983**;7(3):461–467
23. Swanson RA, Schmidley JW. Amnestic syndrome and vertical gaze palsy: early detection of bilateral thalamic infarction by CT and NMR. *Stroke* **1985**;16(5):823–827
24. Buonanno FS, Pykett IL, Brady TJ, et al. Proton NMR imaging in experimental ischemic infarction. *Stroke* **1983**;14(2):178–184
25. Spetzler RF, Zabramski JM, Kaufman B, Yeung HN. Acute NMR changes during MCA occlusion: a preliminary study in primates. *Stroke* **1983**;14(2):185–190
26. Brant-Zawadzki M, Pereira B, Weinstein P, et al. MR imaging of acute experimental ischemia in cats. *AJNR* **1986**;7:7–11
27. Hilal SK, Maudsley AA, Simon HE, et al. In vivo NMR imaging of tissue sodium in the intact cat before and after acute cerebral stroke. *AJNR* **1983**;4:245–249
28. Carr DH, Brown J, Bydder GM, et al. Gadolinium-DTPA as a contrast agent in MRI: initial clinical experience in 20 patients. *AJR* **1984**;143:215–224
29. McNamara MT, Brant-Zawadzki M, Berry I, et al. Acute experimental cerebral ischemia: MRI enhancement using Gd-DTPA. *Radiology* **1986**;158:701–704
30. Gomori JM, Grossman RI, Goldberg HI, Zimmerman RA, Bilaniuk LT. Intracranial hematomas: imaging by high-field MR. *Radiology* **1985**;157:87–93
31. Hart RG, Lockwood KI, Hakim AM, et al. Immediate anticoagulation of embolic stroke: brain hemorrhage and management options. *Stroke* **1984**;15(5):779–789
32. Brant-Zawadzki M, Berry I, Osaki L, Brasch R, Murovic J, Norman D. Gd-DTPA in clinical MR of the brain: I. Intraaxial lesions. *AJNR* **1986**;7:781–788
33. Wisniewski HM, Terry RD. Morphology of the aging brain, human

and animal. In: Ford DE, ed. *Neurobiological aspects of maturation and aging. Progress in Brain Research Series*, vol. 40. New York: Elsevier, **1973**:253–265

34. Peress NS, Kane WC, Aronson SM. Central nervous system findings in a tenth decade autopsy population. In: Ford DE, ed. *Neurobiological aspects of maturation and aging. Progress in Brain Research Series*, vol. 40. New York: Elsevier, **1973**:482–483
35. Bradley WG, Waluch V, Brant-Zawadzki M, Yadley RA, Wycoff RR. Patchy, periventricular white matter lesions in the elderly: a common observation during NMR imaging. *Noninvasive Med Imag* **1984**;1:35–41
36. Melamed E, Lavy S, Bentin S, Cooper YR, Rinot Y. Reduction in regional cerebral blood flow during normal aging in man. *Stroke* **1980**;11(1):31–36
37. Shaw TG, Mortel KF, Meyer JS, Rogers RL, Hardenberg J, Cutaia MM. Cerebral blood flow changes in benign aging and cerebrovascular disease. *Neurology* **1984**;34:855–862
38. Naritomi H, Meyer JS, Sakai F, Yamaguchi F, Shaw T. Effects of advancing age on regional cerebral blood flow. *Arch Neurol* **1979**;36:410–416
39. Humphrey PRD, Marshall J. Transient ischemic attacks and strokes with recovery prognosis and investigation. *Stroke* **1981**;12(6):765–769
40. Brant-Zawadzki M, Fein G, Van Dyke C, Kiernan R, Davenport L, deGroot J. Magnetic resonance imaging of the aging brain: patchy white matter lesions and dementia. *AJNR* **1985**;6:675–682
41. Radda GK, Bore PJ, Rajagopalan B. Clinical aspects of P-31 NMR spectroscopy. *Br Med Bull* **1984**;40:155–159
42. Chance B. Studies of exercise performance, vascular disease, and genetic disease. In: James TL, Margulis AR, eds. *Biomedical Magnetic Resonance.* San Francisco: Radiology Research and Education Foundation, **1984**
43. Horikawa Y, Naruse S, Tanaka C, et al. In vivo ^{31}P NMR studies on experimental cerebral infarction using topical magnetic resonance. *Mag Res Med* **1984**;1(2):169–171